E. Erlbach
R. L. Garwin
M. P. Sarachik

Measurement of Magnetic-Field Attenuation By Thin Superconducting Films

Abstract: The dependence of the field attenuation on temperature and superimposed dc magnetic field is measured with a sensitive rf bridge. It is shown theoretically that the penetration depth λ can be derived from the attenuation measurements, and the experiment therefore yields λ as a function of temperature and dc magnetic field. Changes in λ can be detected to an accuracy of $\pm 0.03\%$. Preliminary data on the temperature dependence of λ for lead are compared with the predictions of the Bardeen-Cooper-Schrieffer theory and are shown to be consistent with an energy gap between $4.9\ kT_c$ and $5.4\ kT_c$ at 0°K. Detailed descriptions are given of the apparatus and of the preparation of the samples.

Introduction

A magnetic field applied to a bulk superconductor produces persistent screening currents which restrict the penetration of the field to a thin layer λ at the surface. Actually, superconductors even *expel* magnetic fields—the Meissner-Ochsenfeld[1] effect. The penetration depth λ has been the subject of many investigations[2-7] and has been shown to vary with temperature and external magnetic field.[8,9] The value of λ at 0°K is of the order of 500 A and increases with temperature. This order of magnitude is predicted by both the London phenomenological theory[10] and the Bardeen-Cooper-Schrieffer[11] microscopic theory. The exact law of penetration of the magnetic field, however, differs in the two theories. For a bulk superconductor the equations of either theory can be solved and the law of penetration derived.[10,11] Although measurements have also been made on bulk superconductors,[3,7,8] it is easier to investigate the penetration depth by using specimens whose dimensions are of the same order of magnitude as the penetration depth itself. Wires,[5] colloids,[4] and thin films[6] satisfy this requirement and have been used for this purpose. A measure of the value of λ can be obtained from such experiments to the same accuracy to which the dimensions of the samples are known. On the other hand, experiments on bulk superconductors detect only changes in λ, and these only as small effects on a large background.

In the present experiment, the measurement of the attenuation of a magnetic field by thin films is used as the method for investigating the penetration depth λ.[12] The attenuation is measured by applying a field on the outside of a cylindrical film and measuring the field which penetrates to the inside.[13] The various theories predict different amounts of penetration, since they use different equations to describe the spatial variation of the field within the superconductor. For the London equations,[10] an exact solution can be derived and is included in the section on theoretical considerations. For the BCS theory the problem is much more difficult. An approximate solution, valid when the film thickness $d \ll \lambda$, has been given by Peter.[14] According to both theories, a thin film shields much more than a corresponding thickness of bulk superconductor.[15] For the London equations, and for $d \ll \lambda$, it will be shown that

$$\frac{H_i}{H_0} = \frac{2\pi\lambda^2}{td}, \tag{1}$$

where H_0 is the magnetic field at the surface of the transmitting side of the film, H_i is the field at the surface of the receiving side of the film, and t is a fundamental length which will be defined later. In this experiment $t = 1$ cm, and thus for $d = 0.5\lambda$, $H_i/H_0 = 4\pi\lambda \approx 6 \times 10^{-5}$. This is to be contrasted with a bulk superconductor, where at a depth of 0.5λ the field would be smaller by a factor of only $e^{-d/\lambda} = 0.6$. Thus very large attenuations are expected for thin films and, to get an accurate measure of the transmitted field, it is important to eliminate all stray leakage of the field around the edges of the film. This is done by winding a coil which produces a space-harmonic

field outside the film, i.e., one which varies sinusoidally in space and which, as a consequence of Maxwell's equations, decreases exponentially with distance from the source. The spatial wavelength of this field is the fundamental dimension t used in Eq. (1). Since an exponentially decreasing field falls off more rapidly than any n-pole field, the space-harmonic field can be well localized in space, and leakage around the film is minimized. Also, the receiving coil, located inside the film, is wound in such a manner that it detects space-harmonic fields and is insensitive to constant fields. The coils are described in more detail in the next section.

In a mutual inductance arrangement such as the one used in this experiment, the sensitivity is directly proportional to the frequency used. A frequency of 2.2 Mc/sec was chosen, since it is high enough to provide adequate sensitivity, and is still below the frequencies where absorption begins to occur in superconductors because of the skin effect or excitations across the energy gap. Therefore, for a superconductor, attenuation measurements at 2.2 Mc/sec are equivalent to dc measurements.

An important consequence of the large attenuation of thin films is the high current density involved in providing this shielding. For sufficiently thin films, the current density is constant throughout the film, and is proportional to H_0/d. The drift velocity with which the superconducting electrons must move in order to provide this current density is thus proportional to H_0/d. As this velocity approaches the velocity of sound in the medium, one would expect to find gradual changes in the superconducting properties of the film, and eventually even elimination of the superconductivity. In order to investigate these effects, an auxiliary solenoid is included in the apparatus which produces a dc magnetic field at the film, and thereby permits measurements of the film attenuation to be made at various drift velocities of the superconducting electrons.

The next three sections discuss the experimental equipment. The last sections of the article are devoted to a discussion of some theoretical considerations and also include some preliminary experimental results.

Coils

The sample and coil arrangement used to measure the attenuation of films is shown in Fig. 1. Cylindrical geometry is used, with the sending coil located outside and the receiving coil located inside the film. A superconducting solenoid wound outside the other coils is used to set up a dc magnetic field. All these are enclosed in a copper shield to reduce stray signals and are immersed in a conventional glass cryostat.

The receiver coil is shown in detail in Fig. 1b. The space-harmonic property is achieved by winding the adjacent series-connected windings in opposite senses, separated by a distance $t/2$, the spatial semiwavelength. The number of windings and the number of turns in each winding, as shown, are chosen to eliminate all dipole and axial quadrupole moments, so that, except for imperfections in winding the coil, the field falls off axially with distance as an octupole. The transmitter coil is wound in the same manner, but on a larger diameter.

Coupling between the miniature coaxial cables which feed the transmitter and receiver coils is reduced by enclosing them in separate grounded inconel tubes. To avoid ground loops, the low-potential ends of the coils are connected to the braids of their respective coaxial cables, and the braids are then grounded at single points outside the cryostat. Spring fingers (not shown in Fig. 1) ground the films through a silver paint underlayer to eliminate electrostatic coupling between the coils. (The silver paint, which insures reliable contact, is applied to the glass substrates before film deposition in the region of the spring fingers.) Residual leakage is measured by replacing the film of Fig. 1 by a copper cylinder of the same length and thick enough to insure that there is no magnetic field penetration through it. With this arrangement the background pickup induced in the receiver coil is less than 10^{-6} of the signal at the transmitter coil.

The solenoid of Fig. 1 produces a uniform axial field in the region of the space-harmonic field but is considerably shorter than the film, so that the screening currents are very small at the film edges.

Preparation of samples

The samples are prepared by evaporating lead or tin in a vacuum of about 10^{-5} mm of Hg onto the outside of cylindrical glass substrates 10.63 cm long, with an inner

Figure 1 **a) Diametral section of sample and coils. b) Receiving coil.**

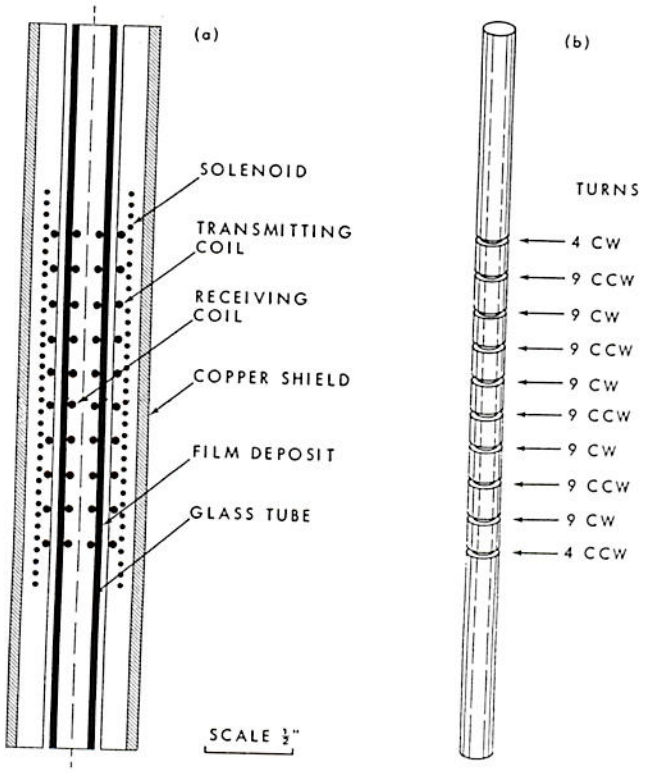

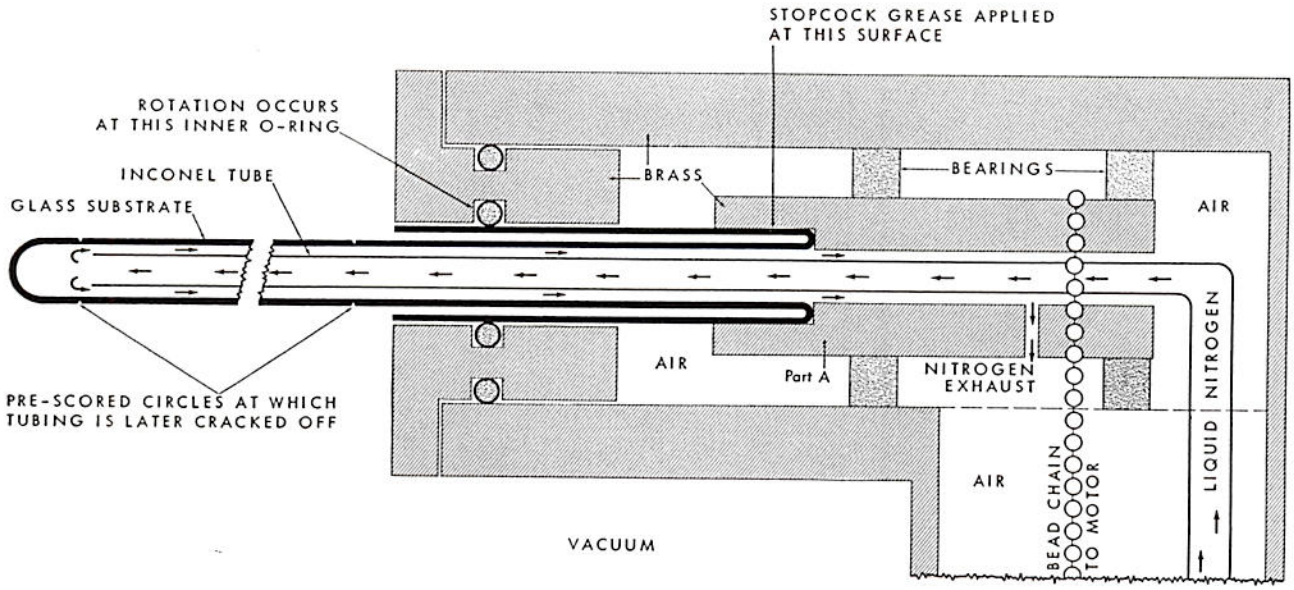

Figure 2 **Schematic diagram of sample rotator for evaporation at liquid-nitrogen temperature.**

diameter of 5 mm and an outer diameter of 7 mm. The glass cylinders are rotated during deposition to insure a uniform coating. Uniformity of the films along the axis is achieved by proper positioning of the source boats. The substrates are cooled to liquid-nitrogen temperature during evaporation and then left to anneal under vacuum at room temperature for about ½ hour. It is realized that these are not films of extreme purity. However, they give very reproducible results and exhibit superconductivity which is just as pronounced as that of bulk metal. Future runs may be taken on films evaporated under cleaner conditions.

The apparatus used for the evaporations is shown in Fig. 2. The glass substrates are prepared from precision tubing in the shape shown, and both ends are split off later, leaving a cylinder 10.63 cm long. Note that the substrates are closed at one end. They are inserted into the rotator, the surface between them and Part A being coated with a mixture of alcohol and glycerin which freezes at nitrogen temperature. The inner O-ring, which serves as a vacuum tight bearing, does not freeze since it is in contact with low temperatures only through the glass, which is a bad heat conductor. Part A is made to rotate by a bead chain which is driven by a motor below. In order to start an evaporation, liquid nitrogen is transferred into the sample through the inconel tube, the back of the sample freezes to the rotator at A, and the sample is rotated.

Film thicknesses were measured using an X-ray fluorescence technique, and were found to be uniform within $\pm 10\%$.

Circuitry

A block diagram of the measuring circuit is shown in Fig. 3. The coil arrangement of Fig. 1 is used as one arm of an rf bridge. The other arm consists of a phase shifter and an accurately calibrated attenuator. The rf phase shifter and attenuator are adjusted to give a null at the bridge output, in which case the two branches of the bridge put out signals of equal amplitude and opposite phase. The ratio of the settings of the attenuator with and without the film in place is therefore a measure of the attenuation of the film.

A doubly coherent system is used for detecting the null, as shown in Fig. 3. A 2.2 Mc/sec signal is modulated by a 400-cps square wave and fed into the rf bridge. The bridge output is added to an unmodulated 2.2-Mc/sec homodyning signal and both are fed into a communications receiver. The coherent rf detection produced by the presence of the relatively large homodyning signal at the diode detector of the communications receiver insures linear operation of that detector. In principle, the steady dc at the diode detector due to the homodyning signal could be subtracted, and the bridge balance would then be indicated by the absence of any additional signal. This is inconvenient, however, since the portion to be subtracted varies with the level of the homodyning signal, with receiver gain, and with detector drift. These difficulties are avoided by modulating the bridge signal and using the resultant ac signal at the detector output of the receiver to indicate the null. This ac signal is fed into a 400 cps phase-coherent (lock-in) detector with a time constant of 0.1 sec.

• *RF source*

The crystal-controlled rf source provides two separate outputs. One is square-wave modulated at 400 cps by a mechanical chopper, while the other output must be unmodulated since it is used as the homodyning signal. These two signals are very well isolated from each other

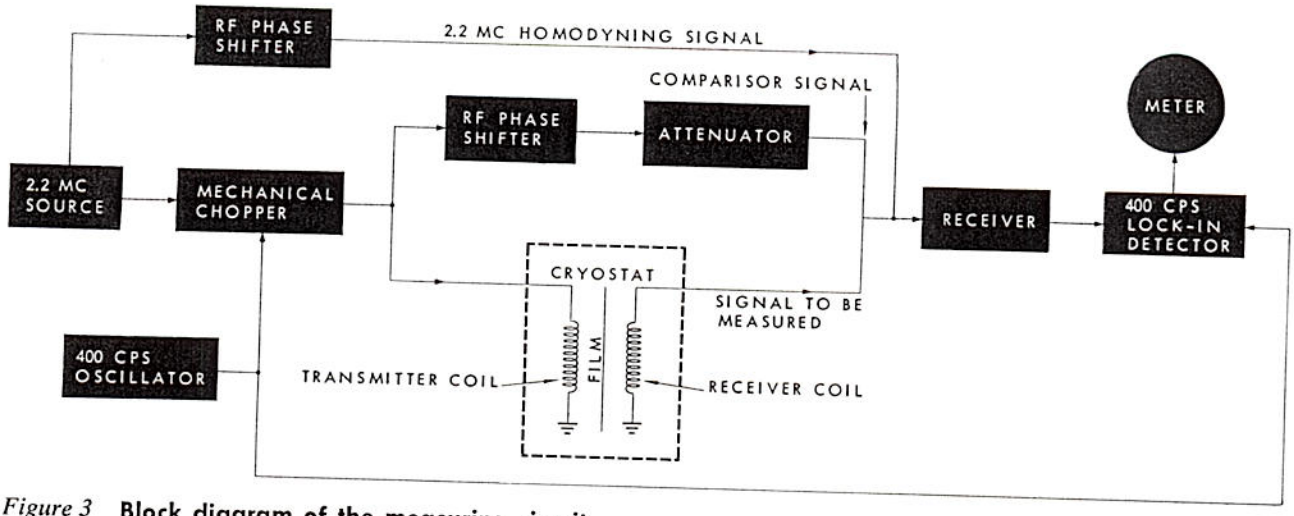

Figure 3 **Block diagram of the measuring circuit.**

to insure that the modulation on the main output does not result in modulation of the homodyning signal.

It is also essential that the rf source be thoroughly shielded so that no stray signal is picked up by one branch of the rf bridge to upset the null balance. The use of shielding techniques equivalent to those employed in the best commercial signal generators was found to be essential. The crystal oscillator and its associated buffer stages and attenuators were each separately enclosed in individual shield cans, whose seams were soldered completely shut wherever necessary. Power leads enter the cans through very well shielded, individual, multisection coaxial rf decoupling circuits. The outer conductors of all rf interstage and output cables were made of several layers of braiding to approximate a solid conducting shield.

• *Attenuator and phase shifters*

An attenuator was specially constructed for this experiment to measure changes in attenuation of $\pm 0.05\%$ and to provide a continuously variable attenuation ratio over a range of 10^4. This attenuator[16] is constructed of two brass pistons which slide inside a brass tube from which they are insulated by teflon spacers (see Fig. 4). The equivalent circuit for this arrangement consists of a small transfer capacitance between the pistons and capacitances to ground from each piston. The transfer capacitance depends on the distance between the pistons and, since the pistons are movable, this capacitance is variable.

The value of the capacitance can be calculated using standard electrostatic methods and can be expressed as

$$C_{\text{transfer}} = \frac{4\pi R}{\varepsilon_0} \sum_{\mu} \frac{1}{m_\mu \sinh(m_\mu d/R)}, \qquad (2)$$

where R = radius of brass tube, ε_0 = permittivity of free space, d = separation of pistons, and the m_μ are the roots of $J_0(m_\mu) = 0$, where J_0 is a zero-order Bessel function. For the dimensions used, all terms in the series except the first are negligible. The capacitance is thus

$$C = \frac{4\pi R}{\varepsilon_0 m_1} \frac{1}{\sinh(m_1 d/R)} = \frac{a}{\sinh kd}, \qquad (3)$$

where $k = \dfrac{2.4042}{R} = 4.341$ in.$^{-1}$.

The attenuation is proportional to $1/C_{\text{trans}}$ since the transfer impedance is very much larger than all other impedances in the circuit. Therefore the attenuation equals $K \sinh kd$, where K depends on the circuit parameters as well as the dimensions of the attenuator. Since only ratios of attenuation with and without the film are measured, the constant K never enters, and need not be known for the experiment. Actually, the coil impedances are slightly changed by the introduction of the film, and this effect is corrected for where necessary.

In the attenuator used here, each piston can travel one inch. The pistons are attached to micrometer heads so that their separation can be accurately measured. With the total travel of two inches between the pistons, the capacitance is calculated to range from 10^{-13} to 10^{-16} farads, giving attenuation ratios from 2.5×10^3 to 1.5×10^7. For smaller attenuations, a series of step attenuators, accurately calibrated by use of the piston attenuator, are inserted in the coil branch of the rf bridge.

The phase shifter in the attenuator branch is a 0.25 μsec variable delay line. To get a full 360-degree phase shift, additional fixed phase shifters are switched in. A delay line is also used in the homodyning signal branch so that the phase of this signal can be varied. This is necessary to insure maximum sensitivity. The attenua-

Figure 4 **Schematic diagram of attenuator.**
Inside diameter of tube is 1.108".

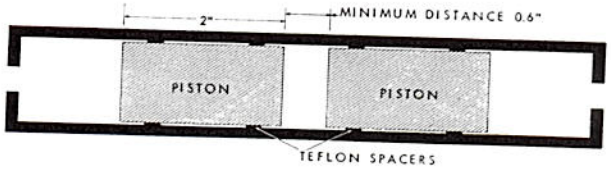

tions of the delay line and the phase shifters are measured where necessary with the piston attenuator.

• *Sensitivity*

Small changes in film attenuations can be reproducibly read to $\pm 0.05\%$, which corresponds to ± 0.0001 in. on the attenuator. As will be shown later, the attenuation varies as $1/\lambda^2$, and thus variations in λ can be measured to $\pm 0.025\%$. Since the penetration depth is of the order of 400 A for lead, this variation corresponds to ± 0.1 A.

Theory

Theoretical predictions for the attenuation of a magnetic field by a thin film can be obtained for the various theories by solving the corresponding field equations within the superconductor subject to the proper boundary conditions. For the London theory[10] the problem can be solved exactly, and this solution will now be derived. A discussion of the solution for the nonlocal theories will be given later.

Consider a superconducting film of thickness d, in the y-z plane. The film is located between $x=0$ and $x=d$. The field is produced in Region I, $x<0$, and is detected by a coil in Region III, $x>d$. In these regions the field must be a solution of Maxwell's equations. Thus, except for the location of the coil itself, the equations can be written as:

$$\nabla \cdot \mathbf{H}=0 \tag{4a}$$

$$\nabla \times \mathbf{H}=0\,. \tag{4b}$$

In Region II, $0<x<d$, the field must be a solution of London's equations. Thus,

$$\nabla^2 \mathbf{H}=\frac{1}{\lambda^2}\mathbf{H} \tag{5a}$$

$$\nabla \cdot \mathbf{H}=0\,. \tag{5b}$$

The boundary conditions are that $\mathbf{H}$ is continuous at the surfaces of the film, and that the field must be bounded in the region $x>d$.

One more boundary condition is necessary before a solution can be found. This condition must introduce a unit of length which is determined by the physical arrangement. For example, if one chooses to work with a uniform magnetic field, then he must avail himself of the cylindrical geometry of the problem. This is done by imposing the boundary condition that the vector potential at the inner surface of the cylinder, A_i, is equal to $H_i\rho/2$, where ρ is the radius of the cylinder (see Smythe,[17] page 263). The fundamental length introduced here is the radius of the cylinder.

Another possibility is to consider an electromagnetic wave impinging on the film. The fundamental length is then the wavelength of the wave, and additional boundary conditions become available since conditions of continuity can be imposed on the electric field also.

A third possibility is to make use of the fact that the field varies sinusoidally in *space*. The fundamental length introduced here is the space wavelength of the field, and the additional boundary condition stems from the fact that the field must have more than one component.

The problem which should actually be solved for this experiment is the case of a space-harmonic electromagnetic wave impinging on a cylindrical film. The time variation of the field can be neglected since its wavelength is much larger than either the radius ρ of the cylinder, or the space-harmonic wavelength t. The lengths ρ and t are comparable, however, and the solution should therefore take the cylindrical geometry into account. The film is approximated by a plane in the present derivation in order to simplify the calculation, although the solution proceeds in a similar manner for the cylindrical case.

With this assumption, the field in Region I, $x<0$, must consist of at least two nonvanishing components. Suppose

$$H_y=f(x)\sin ky\,,$$

$$H_z=0\,.$$

Then, from Eq. 4b,

$$\frac{\partial H_y}{\partial x}=\frac{\partial H_x}{\partial y}\,,$$

$$H_x=-\frac{1}{k}f'(x)\cos ky\,,$$

and from Eq. 4a

$$f''(x)-k^2 f(x)=0\,,$$

$$f(x)=Ae^{kx}+Be^{-kx}\,.$$

Thus, in Region I

$$H_x=\frac{H_0}{2}\cos ky(e^{-kx}-ae^{kx})$$

$$H_y=\frac{H_0}{2}\sin ky(e^{-kx}+ae^{kx}) \tag{6}$$

$$H_z=0\,.$$

Since H_x and H_y must be continuous at $x=0$, both H_x and H_y are of the form $g(x)\cos ky$ and $h(x)\sin ky$ in Region II, $0<x<d$. Substituting in Eq. 5a gives:

$$\frac{d^2g(x)}{dx^2}-k^2g(x)=\frac{1}{\lambda^2}g(x), \qquad \text{(and the same for } h(x)\text{)}$$

for which the solution is

$$g(x)=Ce^{k'x}+De^{-k'x}\,,$$

$$h(x)=Ee^{k'x}+Fe^{-k'x}\,,$$

with $\quad (k')^2=k^2+\frac{1}{\lambda^2}\,.$

Using Eq. 5b gives:

$$k'C=kE\,,$$

$$k'D=-kF\,.$$

Thus, in Region II:

$$H_x = \cos ky\,(Ce^{k'x} + De^{-k'x}),$$
$$H_y = \sin ky\,(k'/k)\,(Ce^{k'x} - De^{-k'x}), \quad (7)$$
$$H_z = 0.$$

In Region III, $x > d$, the field again has the same form as in Region I, except that only the e^{-kx} solution is allowed, since the field must vanish at large x. Thus,

$$H_x = H_i \cos ky e^{-kx},$$
$$H_y = H_i \sin ky e^{-kx}, \quad (8)$$
$$H_z = 0.$$

Now the boundary conditions of continuity at $x=0$ and $x=d$ are imposed. These give four conditions between H_i, C, D, a, and H_0, so that they can all be expressed in terms of H_0. The solution is:

$$\frac{H_i}{H_0} = \frac{2e^{kd}}{[2-(k/k')-(k'/k)]e^{k'd}+[2+(k/k')+(k'/k)]e^{-k'd}}. \quad (9)$$

Since $k = 2\pi$ cm^{-1} (from the geometry of the coils), $1/\lambda \gg k$ giving $k' \approx 1/\lambda$.

Therefore $k'/k \gg k/k'$ and $k'/k \gg 2$, and

$$\frac{H_i}{H_0} = \frac{\lambda k e^{kd}}{\sinh\, d/\lambda}. \quad (10)$$

Since $e^{kd} \approx 1$ and the field behavior is the same with and without the film except in the region of the film itself, the ratio of attenuation readings with and without the film in place is

$$\frac{R_{\text{with}}}{R_{\text{without}}} = \frac{\sinh\, d/\lambda}{2k\lambda}. \quad (11)$$

The factor 2 results from the fact that there is no image field without the film in place, and is exactly equal to 2 only if the coil impedances are independent of the presence of the film. The correct factor can easily be determined experimentally. If $d \ll \lambda$, then

$$\frac{R_{\text{with}}}{R_{\text{without}}} = \frac{d}{2k\lambda^2}. \quad (12)$$

Thus, for a given film of thickness d the attenuation is proportional to $1/\lambda^2$. A calculation using cylindrical geometry (rather than the planar geometry considered above) shows that the attenuation is still proportional to $1/\lambda^2$, although the constant of proportionality is different. This is an important result, since it means that for a given film, the ratio of the attenuations at two different temperatures (i.e., different λ) is independent of the thickness. Also, variations of λ with superimposed dc magnetic fields can be measured without knowledge of the film thickness.

The question arises as to whether the same useful property is obtained from the nonlocal theories. According to the BCS[11] theory, the field equation to be solved for the superconductor is

$$\nabla^2 \mathbf{A}(\mathbf{r}) = \frac{3}{4\pi c \Lambda_T \xi_0} \int \frac{\mathbf{R}[\mathbf{R}\cdot\mathbf{A}(\mathbf{r}')]J(R,T)\,d\mathbf{r}'}{R^4}, \quad (13)$$

where the integral is taken over the entire film.

$\mathbf{A}$ is the vector potential, $\Lambda_T = (4\pi\lambda^2/c^2)$, and $\mathbf{R} = \mathbf{r} - \mathbf{r}'$. $J(R, T)$ is only slightly dependent on temperature and is very nearly equal to $e^{-R/\xi}$, where ξ is the correlation length, that is, the distance over which the motion of the superconducting electrons is correlated. If one substitutes $e^{-R/\xi}$ for $J(R, T)$, one obtains the phenomenological nonlocal theory proposed by Pippard.[18] If in addition $d \ll \lambda$, an approximate solution of this equation found by Peter[14] is valid. The result of this calculation is that

$$\frac{H_0}{H_i} = \frac{3rd^2}{8\lambda^2\xi_0}\left\{\ln\left(\frac{\xi}{d}\right) + 0.423 + \frac{2d}{3\xi} - \frac{d^2}{12\xi^2} \times \left[\ln\left(\frac{\xi}{d}\right) + 2.006\right]\right\}, \quad (14)$$

where r = radius of cylinder,
ξ = correlation length, and
ξ_0 = correlation length in large unstrained sample,

so that the attenuation is once more proportional to $1/\lambda^2$. Actually, this is the first term of a series, the next term being smaller by a factor of the order $(d/\lambda)^2$.

Consequently, for films which are much thinner than λ, so that terms of the order of $(d/\lambda)^2$ can be neglected, all the theories predict an attenuation proportional to $1/\lambda^2$. For films which are thicker, the next term in the series must be included, and the attenuation A (normalized to the attenuation of the film at 0°K) then becomes

$$A = \left(\frac{\lambda_0}{\lambda}\right)^2\left\{1 - \frac{bd^2}{\lambda_0^2}\left[1 - \left(\frac{\lambda_0}{\lambda}\right)^2\right]\right\}. \quad (15)$$

The numerical value of the constant b depends both on the theory and on the geometry assumed for obtaining the solution. Note also that the thickness of the film now appears, although only in second order.

The following procedure has been found to be practicable in analyzing data from some preliminary runs. Solving the preceding equation for λ/λ_0 gives:

$$\frac{\lambda}{\lambda_0} = \frac{1}{\sqrt{A}}\left[1 - \frac{bd^2}{2\lambda_0^2}(1-A)\right]. \quad (16)$$

For two films a and b of different thicknesses, one should get the same λ/λ_0 at equal temperatures. Thus

$$\frac{1}{\sqrt{A_a}}\left[1 - \frac{bd_a^2}{2\lambda_0^2}(1-A_a)\right] = \frac{1}{\sqrt{A_b}}\left[1 - \frac{bd_b^2}{2\lambda_0^2}(1-A_b)\right],$$

where the subscripts refer to the particular film. This allows one to solve for the quantity $B = (bd_a^2/2\lambda_0^2)$ in terms of the experimentally known quantities A_a, A_b and d_a/d_b. All other values of λ/λ_0 for a given film x are then

calculated from the measured attenuation using

$$\frac{\lambda}{\lambda_0} = \frac{1}{\sqrt{A_x}}\left[1-B\left(\frac{d_x}{d_a}\right)^2(1-A_x)\right]. \qquad (17)$$

Note that only relative film thickness need be known for this analysis. The constant B is calculated to make the curves of λ/λ_0 equal for two films of different thicknesses, and should result in identical curves for films of other thicknesses if this procedure is valid.

Preliminary results

The attenuation of films of various thicknesses has been measured as a function of thickness, temperature, and applied dc magnetic field. Only preliminary results are available at present. Typical curves of attenuation vs t^4, ($t \equiv T/T_c$ where T_c is the critical temperature) and vs dc magnetic field are shown in Figs. 5 and 6. These data were taken for lead between 1.4° and 4.2°K. Note that full scale on the ordinate of Fig. 5 represents only a 10% change in attenuation. All points fall on a smooth curve, indicating the considerable accuracy of the measurements.

Curves of λ/λ_0 vs $y \equiv (1-t^4)^{-1/2}$, calculated from the experimental data as discussed in the previous section, are shown in Fig. 7 for four films ranging in thickness by a factor 3. (The film thicknesses were approximately 150 A, 250 A, 350 A and 400 A.) Note that the data from all four films can indeed be represented by a single curve, indicating the validity of the calculation. The theoretical curve[19] of λ/λ_0 vs y predicted by the BCS theory is also plotted in Fig. 7. The parameter which determines this curve is the gap in the energy spectrum of electrons in the superconductor and its variation with temperature. The BCS theory predicts that the energy gap is $3.5kT_c$ at 0°K and decreases continuously to zero at the critical temperature. It can be seen from Fig. 7 that the experimental data do not agree with this prediction. On the other hand, if the energy gap at 0°K is taken to be $4.93kT_c$ and is assumed to have the same temperature variation as predicted by the BCS theory, the theoretical plot of λ/λ_0 vs y shown in Fig. 7 agrees well with the experimental data. Curves for energy gaps of $4.8kT_c$ and $5.05kT_c$ are also shown in Fig. 7 to indicate the effect of small changes in the energy gap on λ/λ_0.

The above analysis is valid only if the films have a correlation length ξ small compared to λ. This is not an unreasonable assumption for our lead films since lead has been found to behave approximately as a London metal.[20] Furthermore, one would expect the correlation length ξ to be limited by the thickness of the films.

If, however, the films have a correlation length ξ which is not small compared to λ, a different analysis is necessary. For the extreme anomalous case, $\xi \to \infty$, the analysis is identical to the foregoing analysis, except that λ must be replaced by $\lambda_\infty^{3/2}$ wherever it appears.[12] A comparison of the experimental data with BCS predictions for $\lambda_\infty^{3/2}$ is shown in Fig. 8 for various energy gaps. It can be seen that the data agree fairly well with the theoretical curve for an energy gap of $5.4kT_c$.

We thus conclude that our data places the energy gap for lead between the values $4.9kT_c$ and $5.4kT_c$. This should be compared with the value of $4.1kT_c$ found by Richards and Tinkham[21] from infrared absorption measurements on lead.

It should be noted that the values of the energy gap presented in this paper are deduced from the experimental data using the BCS theory, and their validity therefore depends on the validity of that theory. Since the BCS theory is admittedly an approximate theory and, in addition, does not apply as well to lead as to more conven-

Figure 5 **Experimental data of normalized attenuation vs t^4.** (*The reduced temperature $t=T/T_c$ is calculated using $T_c=7.22$°K.*)

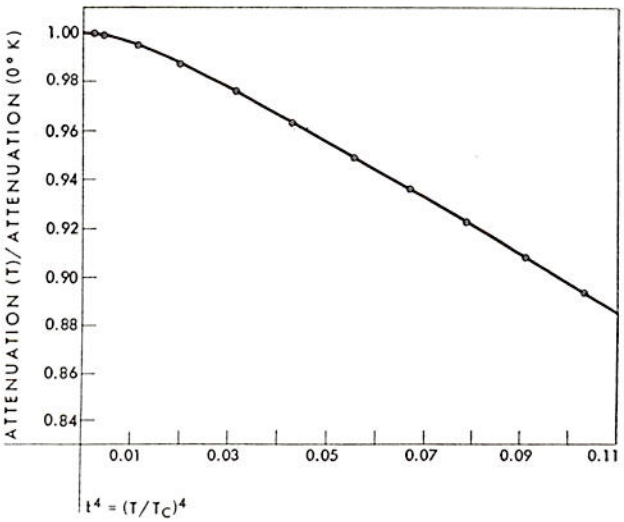

Figure 6 **Attenuation vs dc magnetic field at various temperatures.**

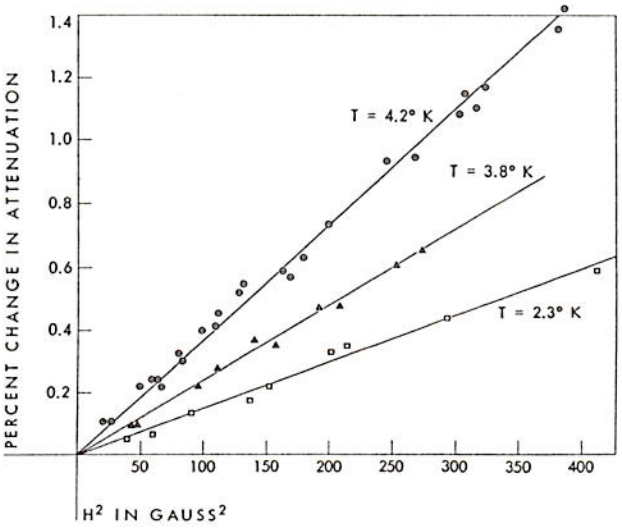

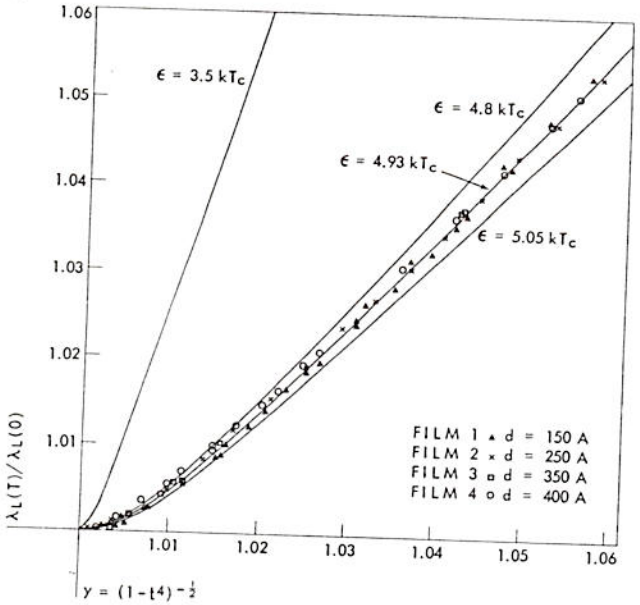

Figure 7 **Comparison of experimental data with theoretical BCS curves of λ_L, for various energy gaps. (Data for lead films.)**

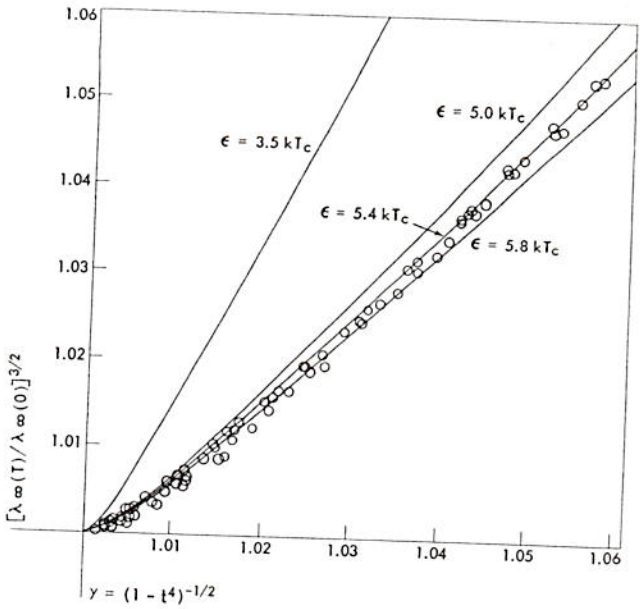

Figure 8 **Comparison of experimental data with theoretical BCS curves of $\lambda_\infty^{3/2}$ for various energy gaps. (Data for lead films.)**

tional superconductors (such as tin and aluminum), the order of magnitude agreement obtained is considered satisfactory.

In the near future the temperature range will be extended to the transition temperature of lead (7.22°K), and down to about 1°K. Data will also be taken on tin at temperatures to 0.5°K.

Limited data have been obtained to date on attenuation as a function of dc field, and the results are still uninterpreted. However, preliminary data (see Fig. 6) indicate that good measurements can be obtained and that the results will be of interest.

Acknowledgments

We would like to express our appreciation to R. J. Blume and A. G. Redfield for many helpful discussions and suggestions. We also thank T. A. Boster, of the IBM General Products Division Development Laboratory, Endicott, for measuring the thickness of our films.

References and footnotes

1. W. Meissner and R. Ochsenfeld, "Ein Neuer Effekt bei Eintritt der Supraleitfähigkeit," *Naturwiss.* **21,** 787-788 (1933).
2. E. Laurmann and D. Shoenberg, "Penetration of Magnetic Field into Superconductors," *Nature* **160,** 747-748 (1947).
3. A. B. Pippard, "The Surface Impedance of Superconductors and Normal Metals at High Frequencies. III," *Proc. Roy. Soc.* **191, A,** 399-415 (1947).
4. D. Shoenberg, "Properties of Superconducting Colloids and Emulsions," *Proc. Roy. Soc.* **175, A,** 49-70 (1940).
5. M. Desirant and D. Shoenberg, "Penetration of Magnetic Fields into Superconductors. I," *Proc. Phys. Soc.* **60,** 413-424 (1948).
6. J. M. Lock, "Penetration of Magnetic Fields into Superconductors. III," *Proc. Roy. Soc.* **208, A,** 391-408 (1951).
7. A. L. Schawlow and G. E. Devlin, "Effect of the Energy Gap on the Penetration Depth of Superconductors," *Phys. Rev.* **113,** 120-126 (1959).
8. A. B. Pippard, "The Surface Impedance of Superconductors and Normal Metals at High Frequencies. IV," *Proc. Roy. Soc.* **203, A,** 98-118 (1950).
9. M. Spiewak, "Magnetic Field Dependence of the Surface Impedance of Superconducting Tin," *Phys. Rev.* **113,** 1479-1494 (1959).
10. F. London, *Superfluids,* Vol. I, John Wiley & Sons, Inc., New York, 1950.
11. J. Bardeen, L. N. Cooper and J. R. Schrieffer, "Theory of Superconductivity," *Phys. Rev.* **108,** 1175-1204 (1957).
12. The penetration depth λ used in this article always refers to the London penetration depth λ_L. It is defined as the distance in which the exponentially decaying field pre-

dicted by the London theory for a bulk superconductor decreases by a factor e. It is analogous to the skin depth δ in normal conductors but differs in two respects: (a) unlike δ, λ_L is frequency independent, and (b) λ_L is not multiplied by a complex factor in the exponential.

The London penetration depth enters the nonlocal theories as a parameter which is defined as above in the limit that the correlation length ξ (the distance in which the motion of the superconducting electrons is correlated) approaches zero. In all other cases ($\xi \neq 0$) the decay is not exponential and λ_L is not a measure of the penetration of the field. For these cases a different quantity λ_a is defined to give a measure of the field penetration. The depth λ_a is a function of λ_L and ξ. In the limit $\xi \gg \lambda_L$, λ_a is proportional to $(\lambda_L)^{2/3}$ and is called λ_∞. In the limit $\xi \ll \lambda_L$, λ_a is equal to λ_L.

13. This method was used by A. L. Schawlow, "Penetration of Magnetic Fields through Superconducting Films," *Phys. Rev.* **109,** 1856-1857 (1958). It is also being used by R. Jaggi and R. Sommerhalder, "Eindringtiefenmessung an Supraleitenden Zinnfilmen" *Helv. Phys. Acta* **32,** 313-314 (1959). See also *Helv. Phys. Acta* **31,** 292 (1958).
14. M. Peter, "Penetration of Electromagnetic Fields through Superconducting Films," *Phys. Rev.* **109,** 1857-1858 (1958).
15. Note that the penetration depth λ is a direct measure of the penetration of a field into a *bulk* superconductor. In a thin film, however, the field falls by a factor e in a distance *much* smaller than the penetration depth. Therefore, λ no longer has the same physical significance, although it still enters into the equations determining the field penetration.
16. This is a standard waveguide beyond cut-off attenuator. See N. Marcuvitz, *Waveguide Handbook,* Rad. Lab. Series, Vol. 10, McGraw-Hill Book Co., Inc., New York, 1951.
17. W. R. Smythe, *Static and Dynamic Electricity,* McGraw-Hill Book Co., Inc., New York, 1950.
18. A. B. Pippard, "The Field Equation of a Superconductor," *Proc. Roy. Soc.* **216, A,** 547-568 (1953).
19. These theoretical curves were calculated for the BCS theory with the aid of tables compiled by B. Muhlschlegel, "Die Thermodynamischen Funktionen des Supraleiters," *Z. Physik* **155,** 317-327 (1959).
20. I. M. Khalatnikov and A. A. Abrikosov, "The Modern Theory of Superconductivity," *Advances in Physics* **8,** 66 (1959).
21. P. L. Richards and M. Tinkham, "Far Infrared Energy Gap Measurements in Bulk Superconductors," *Phys. Rev. Lett.* **1,** 318-320 (1958).

Received November 13, 1959

ENDO